# Transmembrane Segment Peptides Can Disrupt Cholecystokinin Receptor Oligomerization without affecting Receptor Function†

Kaleeckal G. Harikumar, Maoqing Dong, Zhijie Cheng, Delia I. Pinon, Terry P. Lybrand,‡ and Laurence J. Miller*

*Cancer Center and Department of Molecular Pharmacology and Experimental Therapeutics, Mayo Clinic, Scottsdale, Arizona 85259, and Department of Chemistry and Center for Structural Biology, Vanderbilt University, Nashville, Tennessee 37235*

*Received June 3, 2006; Revised Manuscript Received August 24, 2006*

ABSTRACT: Oligomerization of the G protein-coupled cholecystokinin (CCK) receptor has been demonstrated, but its molecular basis and functional importance are not clear. We now examine contributions of transmembrane (TM) segments to oligomerization of this receptor using a peptide competitive inhibition strategy. Oligomerization of CCK receptors tagged at the carboxyl terminus with *Renilla* luciferase or yellow fluorescent protein was quantified using bioluminescence resonance energy transfer (BRET). Synthetic peptides representing TM I, II, V, VI, and VII of the CCK receptor were utilized as competitors. Of these, only TM VI and VII peptides disrupted receptor BRET. Control studies established that the $\beta_2$-adrenergic receptor TM VI peptide that disrupts oligomerization of that receptor had no effect on CCK receptor BRET. Notably, disruption of CCK receptor oligomerization had no effect on agonist binding, biological activity, or receptor internalization. To gain insight into the face of TM VI contributing to oligomerization, we utilized analogous peptides with alanines in positions 315, 319, and 323 (interhelical face) or 317, 321, and 325 (external lipid-exposed face). The $Ala^{317,321,325}$ peptide eliminated the disruptive effect on CCK receptor BRET, whereas the other mutant peptide behaved like wild-type TM VI. This suggests that the lipid-exposed face of the CCK receptor TM VI most contributes to oligomerization and supports external contact dimerization of helical bundles, rather than domain-swapped dimerization. Fluorescent CCK receptor mutants with residues 317, 321, and 325 replaced with alanines were also prepared and failed to yield significant resonance transfer signals using either BRET or a morphological FRET assay, further supporting this interpretation.

Association of membrane proteins within the lipid bilayer is well described (*1*). For the single transmembrane receptor tyrosine kinases, dimerization represents a mechanism for cross phosphorylation and regulation that is critical to their activity (*2*). In recent years, it has also been recognized that the heptahelical G protein-coupled receptors can form dimers and higher order oligomers within the membrane, and this can have profound functional implications (*3*−*5*). Two broad classes of G protein-coupled receptor dimers have been proposed (*6*). In the domain-swapped dimers, the portion of one receptor typically extending from the amino-terminal tail through the fifth transmembrane (TM[1]) segment associates with the complementary portion of another receptor molecule representing the sixth TM segment through the carboxyl-terminal tail. This is made possible by the characteristically long third intracellular loop domains of these receptors. Proof of the ability of such oligomers to exist comes from the expression of two non-functional mixed chimeric or truncated receptors that then become functional upon coexpression (*7*, *8*). These complexes have been demonstrated in model systems in which they are heavily overexpressed. The extent to which these might occur in physiologic settings is not yet clear. The second type of G protein-coupled receptor oligomeric complex occurs through the contact of normally formed heptahelical complexes, presumably through a lipid-exposed face. Evidence for this phenomenon comes from models based on crystal structures, although these have not been adequately robust to provide molecular details or mechanisms (*9*−*11*).

A variety of techniques have been utilized to demonstrate the physical association of receptor molecules (*4*, *12*). Resonance transfer and coprecipitation techniques have been most commonly utilized. Although both of these establish spatial approximation of molecules, neither of these distinguishes one type of complex from the other (domain-swapped vs contact) or the specific face of the helical segment that might be critical. A technique that offers promise for establishing this is the competitive-inhibition technique using peptides representing candidate sequences that was previously reported by Hebert and his colleagues (*11*, *13*). In this, a proximity assay such as bioluminescence resonance energy transfer (BRET) is applied to intact tagged receptors that are known to associate, whereas peptides representing the TM segments are added to the incubation.

† This work was supported by the National Institutes of Health Grant DK32878 (to L.J.M.), the Fiterman Foundation, and the Mayo Foundation.

* Corresponding author. Tel: (480) 301-6650. Fax: (480) 301-6969. E-mail: miller@mayo.edu.

‡ Vanderbilt University.

[1] Abbreviations: $\beta_2$AR, $\beta_2$-adrenergic receptor; BRET, bioluminescence resonance energy transfer; FRET, fluorescence resonance energy transfer; CCK, cholecystokinin; CCKAR, Type A CCK receptor; CHO, Chinese hamster ovary; KRH, Krebs-Ringer-HEPES buffer; Rlu, *Renilla* luciferase; TM, transmembrane; YFP, yellow fluorescent protein.

10.1021/bi061107n CCC: $33.50 
Published on Web 11/17/2006

If the latter corresponds to a segment that is critical for receptor oligomerization, it can compete for that domain and might disrupt the complexes in a competitive manner. Furthermore, the faces of that TM segment can be individually studied by changing key residues within that face of the helical peptide. Ultimately, the hypothesis can be further tested with an intact receptor mutant.

In the current work, we have applied this experimental strategy to the Family A G protein-coupled cholecystokinin (CCK) receptor. We have previously demonstrated that CCK receptors constitutively form homo-oligomers when expressed in cells, with these complexes disrupted by agonist occupation (*14*, *15*). The molecular basis for these complexes is not currently known. We have used our 3D models for the CCK receptor developed previously (*16*) to predict potential helical contact faces and identify residues within those contact faces that might be important in dimerization interactions. Peptides representing transmembrane segments I, II, and V had no effect on CCK receptor BRET, whereas segments VI and VII reduced the BRET signal. This was also confirmed using the saturation BRET approach (*17*). Of particular interest is the fact that the disruption of CCK receptor oligomerization using this experimental approach had no effect on natural agonist binding, biological activity, or receptor internalization.

To gain insight into the face of the CCK receptor TM segment VI contributing to the observed oligomerization, we also utilized analogous peptides incorporating Ala to replace natural residues in positions 315, 319, and 323 in the interhelical face (6.36, 6.40, and 6.44 in the nomenclature of Ballesteros and Weinstein (*18*)) or in positions 317, 321, and 325 in the external lipid-exposed face (6.38, 6.42, and 6.46). The TM VI-Ala$^{317,321,325}$ peptide eliminated the disruptive effect on CCK receptor BRET (again confirmed by saturation BRET), whereas the other mutant peptide behaved like the wild-type TM VI peptide. This suggests that the lipid-exposed face of CCK receptor TM VI most contributes to receptor oligomerization and best supports the external contact dimerization of established seven-helix bundles, rather than domain-swapped dimerization. As further evidence for this, CCK receptor mutants with fluorescent tags were prepared in which residues 317, 321, and 325 were replaced with Ala residues. Indeed, coexpression of these in cells failed to yield a significant BRET signal, supporting the disruption of CCK receptor oligomerization. This was further supported in a complementary morphological FRET assay as well.

## MATERIALS AND METHODS

*Materials*. CCK-8 peptide was purchased from Peninsula Laboratories (Belmont, CA). Fura-2AM was from Invitrogen (Carlsbad, CA); fetal clone II culture medium supplement was from Hyclone laboratories (Logan, UT); and coelenterazine *h* was from Biotium (Hayward, CA). Other reagents were analytical grade.

*Preparation of CCK Receptor Constructs*. CCK receptor constructs tagged at the carboxyl terminus with either *Renilla* luciferase (Rlu) or yellow fluorescent protein (YFP) were used as donor and acceptor, respectively, for BRET studies. A CFP-tagged CCK receptor was also prepared as a donor for FRET studies. This (pECFP-CCKAR-CFP) was created by incorporating the CCK receptor sequence in frame into the NheI and NotI sites of the pECFP-N1 vector (BD Bioscience Clontech, Palo Alto, CA). We have previously validated the binding and biological activity of the Rlu- and YFP-tagged receptor constructs when transiently expressed in COS cells (*14*). The CFP-tagged CCK receptor construct also behaved in a manner similar to that of the wild-type CCK receptor with respect to its binding affinity and biological activity (data not shown). We also prepared mutants of these receptors in which alanine residues (Ala) were introduced into predicted TM segment VI in positions 317, 321, and 325 using the QuikChange Site-Directed Mutagenesis Kit (Stratagene, La Jolla, CA). The oligonucleotide primers represented the following: sense primer, 5′-GATCCGCATGCTCGCTGTCATCGTGGCC-CTCTTCTTCGCGTGCTGCTGGATGC-3′; antisense primer, 5′-GCATCCAGCACGCGAAGAAGAGGGCCAC-GATGACAGCGAGCATGCGGATC-3′. All receptor sequences were verified by direct DNA sequencing.

*Synthesis of CCK Receptor Transmembrane Segment Peptides*. We synthesized a series of peptides representing the predicted TM segments of the CCK receptor as well as variants of TM VI (Figure 1A). The rationale for the two variants of TM VI in which two distinct faces of this segment were modified was based on our current molecular model of this receptor (*16*) (Figure 1B). The external lateral view of the helical bundle shows that TM VI residues 317, 321, and 325 form a continuous, fully exposed surface patch on the outer face of the helix. In contrast, TM VI residues 315, 319, and 323 are largely buried in the TM VI/TM VII interface, with only small, discontinuous patches visible at the bottom of a deep groove on the helix bundle surface.

Peptides were synthesized as carboxyl-terminal amides using manual solid-phase techniques with a Pal resin (Advanced Chem Tech) and Fmoc-protected amino acids (*19*). The protected amino acids were dissolved in dimethyl formamide and added with the coupling reagents *O*-benzotriazole-*N*,*N*,*N*′,*N*′-tertamethyl uronium hexafluorophosphate and 1-hydroxybenzotriazole added in *N*′, *N*-diisopropylethylamine. The reactions were continued until the ninhydrin tests were negative to be certain of the completion of the reactions. If after 2 h the reactions were still incomplete, then coupling was repeated with fresh reagents. The completed peptides were removed from the resin using a trifluoroacetic acid mixture containing 82.5% (v/v) trifluoroacetic acid, 5% (w/v) phenol, 5% (v/v) distilled water, 5% (v/v) anisole, and 2.5% (v/v) triisopropylsilane for 2 h. These were then filtered, and the resin was washed with trifluoroacetic acid and methylene chloride. The combined filtrates were evaporated and precipitated with ether. The crude peptide products were then dissolved in an ~50% acetonitrile/water mixture, lyophilized, and purified to homogeneity using semipreparative reversed-phase HPLC. Peptides were solubilized in dimethyl sulfoxide and diluted to the required concentrations in Krebs-Ringers-HEPES (KRH) medium (25 mM HEPES at pH 7.4, 104 mM NaCl, 5 mM KCl, 2 mM $CaCl_2$, 1 mM $KH_2PO_4$, and 1.2 mM $MgSO_4$) to yield a final concentration of dimethyl sulfoxide of 1%.

*Cell Culture and Transfection*. Membranes prepared from Chinese Hamster Ovary (CHO) cells stably expressing type A CCK receptors (CHO-CCKAR cells) were used as a source of receptor for radioligand binding studies. Intact CHO-

A

| Receptor | Segments | Sequences |
|---|---|---|
| CCKAR | TMI | EWQSALQILLYSIIFLLSVLGNTLVITV |
| | TMII | FLLSLAVSDALMLCLFCMPFNL |
| | TMV | QTFLLLILFLLPGIVMVVAYGL |
| | TMVI | VIRMLIVIVVLFFLCWMPIFSANAWRA |
| | TMVII | PISFILLLSYTSSCVNPIIYCFM |
| | TMVI-Ala$^{315,319,323}$ | VIRALIVAVVLAFLCWMPIFSANAWRA |
| | TMVI-Ala$^{317,321,325}$ | VIRMLAVIVALFFACWMPIFSANAWRA |
| $\beta_2$AR | TMVI | GIIMGTFTLCWLPFFINIVH |

B

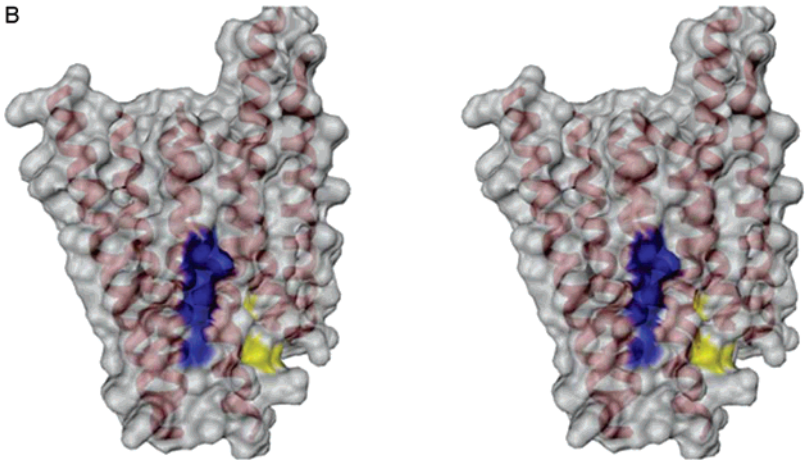

FIGURE 1: Transmembrane segment peptides and CCK receptor surface model. Panel A illustrates the sequences of the CCK receptor and $\beta_2$-adrenergic receptor TM segment peptides utilized in this series of studies, with underlined mutated residues. The exposed surface for the type A CCK receptor is shown in panel B, on the basis of our earlier 3D model (*16*). The amino- and carboxyl-terminal regions have been deleted to focus on the transmembrane domain. A translucent surface was rendered, and TM helices are shown in red for reference. The surface patches for residues 317, 321, and 325 are displayed in blue, whereas the surface patches for residues 315 and 319 are highlighted in yellow (residue 323 is completely inaccessible in this surface representation). The Figure was generated with DINO (*47*), and the surface calculations were performed using MSMS (*48*).

CCKAR cells were used for functional studies of intracellular calcium responses. COS cells were used for the expression of Rlu- and YFP-tagged CCK receptor constructs for BRET studies. For transient transfections, COS cells were plated in 10 cm tissue culture dishes at a density of $0.5 \times 10^6$ cells/dish in Dulbecco's modified eagle's medium supplemented with 5% fetal clone II, 24 h before transfection. The cells were transfected with approximately 3 $\mu$g of total DNA (representing a single construct or the combination of two constructs) per dish using DEAE-dextran (*20*). We previously monitored the levels of expression of these constructs in COS cells using radioligand binding and Western blotting techniques (*14*). Forty-eight to 72 h after transfection, the cells were used for radioligand binding, biological activity assays, BRET, or morphological FRET studies.

*Preparation of Cell Membranes*. A particulate preparation enriched in plasma membranes was isolated from CHO-CCKAR cells using the previously established density gradient centrifugation procedure (*21*). The membranes were suspended in KRH buffer containing 0.01% soybean trypsin inhibitor and 1 mM phenylmethylsulfonyl fluoride and stored at −80 °C until further use.

*Radioligand Binding Assay*. Receptor binding characterization was performed using either CCK receptor-bearing CHO-CCKAR cell membranes or intact COS cells expressing mutant tagged receptor constructs (*22*). The source of receptor was incubated with 1−2 pM CCK-like radioligand ($^{125}$I-D-Tyr-Gly-[(Nle$^{28,31}$)CCK-26-33], specific radioactivity 2000 Ci/mmol) in the absence or presence of unlabeled CCK (concentrations up to 1 $\mu$M) for 1 h at room temperature in KRH at pH 7.4, containing 0.2% bovine serum albumin and 0.01% soybean trypsin inhibitor. Selected assays included TM peptides at a concentration of approximately 1 $\mu$g/mL, representing molar concentrations between 0.3 and 0.5 $\mu$M for the various peptides. For membrane-binding assays, the bound radioligand was separated from free radioligand using a Skatron cell harvester (Molecular Devices, Sunnyvale, CA) with receptor-binding filtermats. For cell-binding assays, bound and free radioligands were separated by two cycles of repeated washing with ice-cold buffer. After aspiration of the medium, the cells were lysed with 0.5 N sodium hydroxide for 30 min at room temperature. Receptor-bound radioactivity was quantified using a gamma spectrometer. Non-saturable binding evaluated in the presence of 1 $\mu$M CCK represented less than 15% of total binding. Data were analyzed using the LIGAND program (*23*) and were plotted using the nonlinear least-squares curve-fitting routine in Prism (GraphPad 4.0, San Diego, CA).

*Measurement of Intracellular Calcium Release*. The ability of receptor-bearing COS or CHO-CCKAR cells to respond

to CCK was determined using an assay for intracellular calcium concentration that has previously been fully characterized (*22*, *24*). In brief, CCK receptor-bearing cells were lifted from the culture plasticware using a nonenzymatic cell dissociation medium (Sigma, St. Louis, MO) and incubated with 5 $\mu$M Fura-2AM in a serum-free medium at 37 °C for 20 min, followed by washing and re-suspension in ice-cold KRH. Cells were then incubated with 1 $\mu$g/mL of the TM peptides for 2 h at 4 °C. In each assay, approximately 2 million cells were stimulated with increasing concentrations of CCK at 37 °C, and fluorescence intensities were measured in a SPEX Fluoromax-3 spectrofluorometer (SPEX Industries, Edison, NJ) using a multigroup acquisition profile in Datamax-3 software. Signal acquisition was collected over 300 s with 5 s increments at an integration rate of 0.05 nm/s. Emission intensities were measured at 520 nm after excitation at 340 and 380 nm, and calcium concentrations were calculated from the ratios of these intensities (*25*). The peak intracellular calcium concentrations were utilized to determine the agonist concentration-dependency of this biological response.

*Receptor Internalization Studies*. Receptor internalization studies were performed in two ways, one following the internalization of fluorescently tagged agonist ligand occupying the receptor and the other following the fluorescently tagged receptor itself. The former was performed as described previously (*26*). CHO-CCKAR cells were grown on coverslips for 48 h and washed twice with ice-cold phosphate buffered saline (PBS) at pH 7.4, supplemented with 0.08 mM $CaCl_2$ and 0.1 mM $MgCl_2$. The cells were incubated with 50 nM Alexa$^{488}$-CCK-8, a fully active fluorescent analogue of CCK (*22*), in the absence or presence of TM segment peptides at 4 °C for 1.5 h. After incubation, the cells were washed with ice-cold PBS and incubated further with pre-warmed PBS at 37 °C for various time points, followed by 2% paraformaldehyde fixation. Coverslips were then washed twice with PBS and mounted on slides using Vectashield (Vector Laboratories, Burlingame, CA), and observed on a Zeiss (Thornwood, NY) Axiovert 200M epifluorescence inverted microscope using the 100 × 1.4 numerical aperture oil objective. The Alexa fluorescence was observed using the FITC filter set with excitation (480/40 nm) and emission (515 nm, long pass (lp)) with a dichroic mirror (505 nm, lp) (Chroma Technology Corp., Rockingham, VT). The images were collected with an Axiocam MRC camera using Axiovision 3.1 software utilizing an autoexposure adjustment with gain 2. The images were then processed to remove the background signal present outside of cells, and final figures were prepared using Adobe Photoshop version 7.0.

For the analysis of the internalization of the fluorescently tagged CCK receptor, the CHO cells stably expressing CCKAR-YFP were used in an analogous manner, occupying the receptor with 100 nM unlabeled, nonfluorescent CCK. The CCKAR-YFP-expressing CHO cells had entirely normal binding of CCK ($K_i = 0.91 \pm 0.15$ nM) and CCK-stimulated intracellular calcium response ($EC_{50} = 0.07 \pm 0.02$ nM CCK). A Zeiss LSM510 confocal microscope (Thornwood, NY) was used to capture the YFP fluorescence. Images were collected after excitation at 488 nm using an argon laser and with emission coming through a 505 nm long pass filter (pinhole diameter of 210 $\mu$m with a plan-apochromat 63 × 1.3 numerical aperture oil objective).

*BRET Studies*. Bioluminescence and fluorescence measurements were performed using approximately 1−2 million receptor-bearing COS cells in suspension in a 1 mL cuvette, as previously described (*14*). Briefly, 48 h after transfection, COS cells were detached using nonenzymatic cell dissociation solution and were subsequently washed with KRH and used for BRET assay. The assay was started by adding the cell-permeant substrate specific for *Renilla* luciferase, coelenterazine *h*, to the cell suspension to yield a final concentration of 5 $\mu$M. The bioluminescence emission spectra from 400 to 600 nm were acquired immediately in a SPEX FluroMax-3 spectrofluorometer using wavelength increments of 2 nm and an integration time of 2 s. YFP fluorescence emission was collected from 500 to 580 nm after excitation at 480 nm. For peptide effects, the transfected COS cells were incubated with 1 $\mu$g/mL of the TM segment peptides for 2 h at 4 °C before performing the BRET assay. The BRET ratio was defined as ((emission at 510−590 nm) − (emission at 440−500 nm) × Cf)/(emission at 440−500 nm), where Cf corresponds to (emission at 510−590 nm)/(emission at 440−500 nm) for the CCKAR-Rlu construct expressed alone in analogous experiments.

For further characterization of the BRET signal, saturation BRET experiments were performed (*17*). For these, dishes of COS cells were transiently cotransfected with a fixed amount of the Rlu-tagged CCK receptor construct (1.5 $\mu$g DNA/dish) and with increasing amounts of YFP-tagged CCK receptor construct (0.3 $\mu$g to 6 $\mu$g DNA/dish). Forty-eight hours after transfection, cells were detached using a cell dissociation medium and were used for BRET assays, as described above. Fluorescence and luminescence intensities were collected from the same populations of cells used for the BRET studies. There was a linear relationship observed between the intensities (luminescence or fluorescence) and the quantity of receptor expressed. Background-subtracted fluorescence and luminescence intensities were collected to calculate the acceptor-to-donor ratios that were plotted against the BRET ratios (*17*). The Rlu luminescence and YFP fluorescence represent relative intensity values for expressed donor and acceptor proteins, respectively. The total luminescence intensity of the donor was measured between 440 and 500 nm after the addition of 5 $\mu$M coelenterazine *h* using a SPEX FluroMax-3 spectrofluorometer. The total fluorescence intensity of the acceptor was measured by exciting it at 480 nm and collecting emission between 500 and 570 nm. Curves were fit to these data and evaluated for quality of fit based on $R^2$ values (GraphPad 4.0, San Diego, CA). When a single phase exponential curve was significantly better than a linear function (F test determination with $p$ value $<0.05$), it was utilized to calculate $BRET_{max}$ and $BRET_{50}$ values.

*Morphological FRET Microscopy*. Morphological FRET microscopy was performed as described previously (*27*). In short, COS cells were plated in 10 cm tissue culture dishes at a density of $0.5 \times 10^6$ cells/dish. These were transfected using 1.5 $\mu$g of each CFP- and YFP-tagged CCK receptor constructs. Approximately 24 h after transfection, cells were washed and lifted from the dishes and seeded onto 25 mm sterilized coverslips. FRET imaging was performed using an Axiovert 200M inverted microscope (Carl Zeiss, Thornwood, NY) equipped with a dedicated epifluorescence filter set (Chroma Technology Corp., Brattleboro, VT) for CFP

(excitation, 436/20 nm; dichroic mirror, 455 nm, dclp; and emission, 480/40 nm), YFP (excitation, 500/20 nm; dichroic mirror, Q515 lp; and emission, 535/30 nm), and FRET (excitation, 436/20 nm; dichroic mirror, 455 nm, dclp; and emission, 535/30 nm). Images were collected separately for each of the three channels with a constant exposure time (10−250 ms with no binning) using a monochromatic ORCA-12ER CCD camera (Hamamatsu, Bridgewater, NJ) with automated QED-InVivo 2.0 acquisition software (Media Cybernetics Inc., Silver Spring, MD). FRET images were corrected for donor or acceptor bleed-through into the FRET channel by the sensitized-emission method provided by Metamorph version 6.3 (Molecular Devices, Sunnyvale, CA). Corrected FRET, $FRET_c$ = FRET − ($B$ × CFP) − ($A$ × YFP) where FRET, CFP and YFP represent the background-subtracted images (pixel intensity generated from noise outside of the cells that was related to the camera and the filter were removed) collected in the respective channels. $B$ and $A$ represent coefficients for bleed-through into the FRET channel of the donor (CFP) and acceptor (YFP). The bleed-through coefficients used here were similar to those we have described previously in analogous assays (*27*). Final images were assembled and organized using Adobe Photoshop version 7.0.

*Statistical Analysis*. The level of significance of the BRET data were analyzed using the Student's *t*-test for unpaired values. Significant differences were considered to be at the $p < 0.05$ level.

## RESULTS

*Role of Transmembrane Segment Peptides in CCK Receptor Oligomerization*. A series of studies was focused on evaluating the potential role of the transmembrane regions of the CCK receptor in receptor oligomerization. The precedent for this approach comes from studies focused on the $\beta_2$-adrenergic receptor ($\beta_2$AR), in which a peptide corresponding to TM segment VI inhibited receptor dimerization and agonist-dependent stimulation of adenylate cyclase activity (*13*). We have synthesized a series of peptides corresponding to TM segments I, II, V, VI, and VII of the CCK receptor (Figure 1A). We also synthesized peptides that replaced the natural residues in positions 315, 319, and 323 (interhelical face) (designated TM VI-Ala$^{315,319,323}$) or in positions 317, 321, and 325 (external lipid-exposed face) (designated TM VI-Ala$^{317,321,325}$) of TM VI with Ala residues (Figure 1A and B). For control studies, we also synthesized the peptide corresponding to the TM VI segment of the $\beta_2$-AR (Figure 1A). Cells coexpressing Rlu- and YFP-tagged CCK receptor constructs were incubated with the TM segment peptides and were used in BRET assays. Figure 2A includes a series of controls that helped to establish the level of BRET signal that was significant, and that was attributable to background. A strong BRET signal (0.24) was observed in cells expressing a Rlu-YFP fusion protein (positive control), whereas cells coexpressing Rlu- and YFP-tagged CCK receptors produced a significant BRET signal (0.08) above the background, nonspecific signal (0.026) obtained from cells expressing the Rlu-tagged CCK receptor along with soluble YFP or in cells expressing the YFP-tagged CCK receptor along with soluble Rlu. Figure 2B shows that peptides corresponding to CCK receptor TM segments I, II, and V had no effect on the CCK receptor BRET signal,

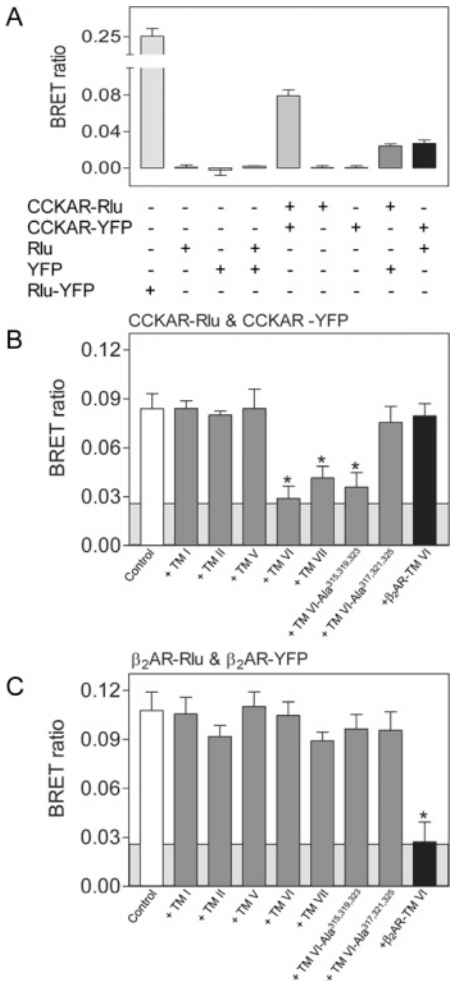


FIGURE 2: Effects of receptor TM segment peptides on CCK receptor BRET. Shown are BRET ratios obtained from a series of control experiments performed in COS cells expressing various combinations of constructs as indicated (A) or transfected with both fluorescently tagged CCK receptors (B) or $\beta_2$-adrenergic receptors (C) after incubating with peptides corresponding to TM segments of the CCK receptor or the $\beta_2$AR. Cells were incubated with 1 $\mu$g/mL of peptide and studied by BRET. TM VI-Ala$^{315,319,323}$ represents the peptide sequence of CCK receptor TM VI with M$^{315}$, I$^{319}$, and F$^{323}$ each mutated to Ala, and TM VI-Ala$^{317,321,325}$ represents the peptide sequence of CCK receptor TM VI with I$^{317}$, V$^{321}$, and L$^{325}$ mutated to Ala. The shaded area represents the nonspecific BRET signal that can be generated from the Rlu-tagged receptor vs the soluble YFP protein or from the YFP-tagged receptor vs the soluble Rlu (0.026), with BRET signals above this area considered to be significant. Data are presented as the means ± S.E.M. of five independent experiments. *$p < 0.05$ compared with the BRET signal obtained for the same receptor-expressing cells incubated without the TM peptide as the control.

whereas CCK receptor TM segments VI and VII significantly reduced this signal. It is important to note that these TM segment peptides reduced the BRET signal to the level consistent with the background generated by the coexpression of the receptor with the soluble partner fluorophore. These data suggest that this receptor−oligomeric complex was essentially fully disrupted (90−95%) by these peptides. None of the CCK receptor peptides had any effect on the BRET signal from the $\beta_2$AR (Figure 2C). The TM VI peptide from the $\beta_2$AR had its reported effect on $\beta_2$AR BRET (Figure 2C), while having no effect on CCK receptor BRET (Figure 2B).

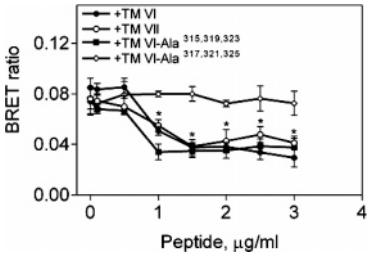


FIGURE 3: Concentration dependency of TM peptides on CCK receptor BRET. Shown are the BRET ratios obtained after cells were incubated with various concentrations of peptides corresponding to CCK receptor TM VI, TM VII, and mutant peptides of TM VI. The BRET ratio is dependent on the concentration of peptide used in the assay. The BRET ratio was significantly decreased with 1 $\mu$g/mL of peptide, even with higher concentrations. Data are represented as the means ± S.E.M. of five independent experiments. *$p < 0.05$ compared with the BRET signal from the same cells without incubating with peptide.

*Analysis of the Relevant Face of TM Segment VI Peptide in Affecting CCK Receptor Oligomerization*. Additional studies were performed to further refine insights into which face of the CCK receptor TM VI was most important for CCK receptor oligomerization. For this, we studied two peptides corresponding to this segment with the native residues on one face changed to Ala residues (Figure 1A). Here, incubation with the peptide representing TM VI-Ala$^{315,319,323}$ (interhelical face modified) yielded the same results as the wild-type TM VI peptide, disrupting the receptor BRET signal (Figure 2B). In contrast, the peptide corresponding to this segment with the lipid-exposed external face modified, TM VI-Ala$^{317,321,325}$, had no effect on the receptor BRET signal, eliminating the disruptive effect of the natural TM VI peptide (Figure 2B). Of note, the 1% dimethyl sulfoxide that was used to solubilize and to deliver the TM peptides to the assay system did not have any effect on the receptor BRET signal, with these two controls not different from each other. Similarly, none of the CCK receptor TM peptides had any effect on the dimerization of the $\beta_2$-adrenergic receptor (Figure 2C). Figure 3 shows that the disruption of receptor oligomerization by each peptide that had an effect on receptor BRET was concentration-dependent.

*Functional Effects of CCK Receptor Oligomerization*. The ability to disrupt CCK receptor oligomerization by incubation with selected TM peptides provided a powerful tool to examine the function of CCK receptor oligomerization. We used this to study CCK radioligand binding, CCK-stimulated intracellular calcium concentrations, and agonist-stimulated CCK receptor internalization. Figure 4 shows that receptor TM peptides that disrupted the oligomerization of the CCK receptor had no effect on CCK radioligand binding. The binding of CCK was similar in all cases. The $K_i$ values (nM) were the following: control, 0.52 ± 0.08; in the presence of TM VI, 0.54 ± 0.16; TM VII, 0.65 ± 0.06; and TM VI-Ala$^{315,319,323}$, 0.34 ± .07). The $B_{max}$ values (pm/mg protein) were the following: control, 4.2 ± 1.7; in the presence of TM VI, 4.3 ± 2.4; TM VII, 4.9 ± 1.3; and TM VI-Ala$^{315,319,323}$, 3.9 ± 2.2. These observations demonstrate that CCK receptor oligomerization had no influence on natural ligand binding, with no apparent change in binding affinity or number of accessible sites.

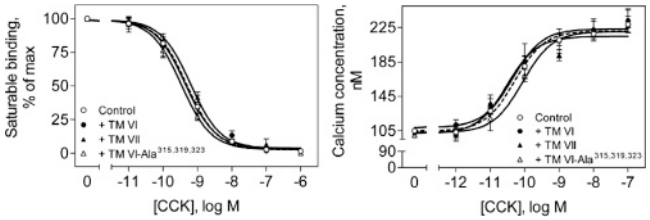


FIGURE 4: Binding and biological activity of the CCK receptor in the presence of TM peptides. Shown are competition binding curves for CCK binding to CHO-CCKAR membranes after incubation with CCK receptor TM peptides (left panel). The $K_i$ and $B_{max}$ values for CCK binding under these conditions are listed in Results. Shown also are the intracellular calcium concentrations in response to CCK in CHO-CCKAR cells pretreated with CCK receptor TM peptides (right panel). Incubations with the TM peptides did not have any effect on CCK binding or CCK-stimulated biological activity. The values represent the means ± S.E.M of data from three independent experiments performed in duplicate.

The CCK receptor is normally coupled to G*q* and activates a signaling cascade that includes phospholipase C and the release of intracellular calcium. Incubation of the TM peptides with CHO-CCKAR cells also had no effect on CCK-stimulated release of intracellular calcium. Figure 4 shows that the peptides that disrupt the formation of receptor oligomers did not have any effect on intracellular calcium signaling. The calcium response parameters were similar in all conditions ($EC_{50}$ values (nM): control, 0.082 ± 0.006; in the presence of TM VI, 0.068 ± 0.018; TM VII, 0.058 ± 0.004; and TM VI-Ala$^{315,319,323}$, 0.073 ± 0.003). This also proves that CCK receptor signaling does not depend on receptor oligomerization.

We previously demonstrated that agonist occupation stimulates CCK receptor internalization (*26*). Figure 5 shows that the disruption of CCK receptor oligomerization using selected TM peptides also did not affect agonist-stimulated CCK receptor internalization. Internalization studies were performed both following the fluorescently tagged agonist ligand occupying the receptor (Figure 5A) and following the fluorescently tagged receptor directly (Figure 5B). Both yielded similar results, with no interference observed upon the disruption of the oligomeric complexes.

*BRET with Mutant CCK Receptors*. The TM peptide co-incubation studies suggested that the lipid-exposed external face of TM VI was critical for CCK receptor oligomerization. In this series of studies, we extended and tested that hypothesis directly using a mutant CCK receptor in which the same residues predicted to be exposed to the lipid, I$^{317}$, V$^{321}$, and L$^{325}$, were mutated to Ala residues. We also prepared CFP-, Rlu-, and YFP-tagged versions of this construct to explore their oligomerization status in BRET and in FRET imaging studies.

First, it was critical to be certain that such CCK receptor mutants functioned normally. Indeed, these constructs were shown to normally bind CCK and to signal in response to CCK (Figure 6). Figure 6 also shows that Rlu- and YFP-tagged mutant CCK receptors that were used in the BRET studies were able to bind CCK specifically with high affinity, similar to the untagged wild-type CCK receptor. The binding affinity for CCK was similar to that of the wild-type receptor ($K_i$ values (nM): WT CCKAR, 1.0 ± 0.1; CCKAR-Ala$^{317,321,325}$-Rlu, 2.8 ± 0.9; and CCKAR-Ala$^{317,321,325}$-YFP, 2.1 ± 0.9). Intracellular calcium responses to CCK were also

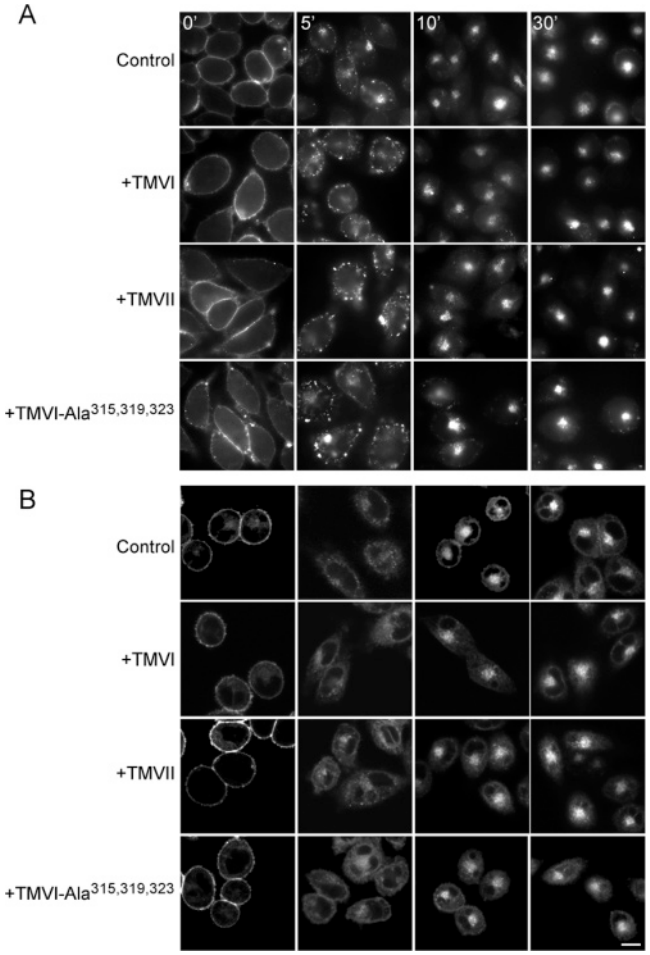


FIGURE 5: Time course of agonist-induced internalization of CCK receptor in the presence of CCK receptor TM peptides. Shown are representative microscopic images demonstrating CCK receptor internalization in Alexa$^{488}$-CCK occupied CHO-CCKAR cells (A) or unlabeled CCK bound to YFP-tagged CCK receptors expressed on CHO cells (B) after incubation with CCK receptor TM peptides. Cells were incubated with 50 nM of the Alexa$^{488}$-CCK ligand or 100 nM CCK for 1.5 h at 4 °C to saturate surface receptors. Receptor internalization was then monitored over time in response to warming in the presence of the TM peptides. Using both techniques, the CCK receptor was shown to be similarly internalized in the presence and absence of the TM peptides. Scale bar represents 20 $\mu$m.

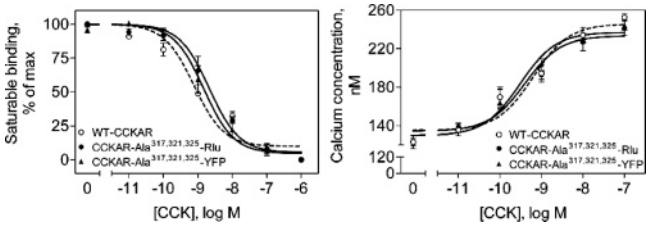


FIGURE 6: Functional characterization of fluorescently tagged CCK receptor mutants. Shown are the concentration-dependent curves representing CCK binding (left panel) and intracellular calcium responses to CCK in tagged mutant CCK receptor-bearing COS cells (right panel). Both tagged triple-Ala mutant CCK receptors behaved in a manner similar to that of the wild-type receptor in binding and biological activity. The $K_i$ values for these studies are listed in Results. Calcium concentrations are expressed as absolute values (nM). Data are represented as the means ± S.E.M of three independent experiments performed in duplicate.

similar to those of the wild-type CCK receptor (Figure 6). The $EC_{50}$ values (nM) were as follows: WT CCKAR, 0.87 ± 0.05; CCKAR-Ala$^{317,321,325}$-Rlu, 1.02 ± 0.24; and CCKAR-Ala$^{317,321,325}$-YFP, 2.1 ± 0.8. Of note, the CFP-tagged mutant CCK receptor that was used in the morphological FRET imaging studies also behaved in a manner similar to that of the wild-type CCK receptor with respect to its binding affinity and biological activity (data not shown).

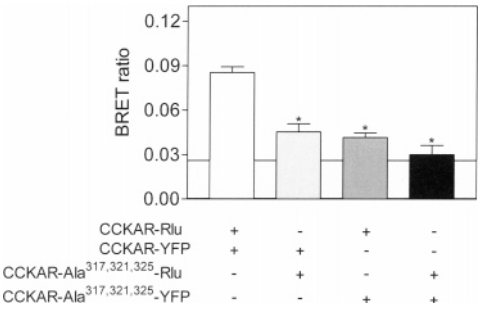


FIGURE 7: Impact of CCK receptor mutation on the BRET signal. Shown are the BRET ratios obtained from COS cells coexpressing Rlu- and YFP-tagged CCK receptor constructs. Included are the wild-type CCK receptor and a mutant CCK receptor construct in which three amino acids on the predicted lipid-exposed external face of TM segment VI were mutated to alanines ($I^{317}$, $V^{321}$, and $L^{325}$ to Ala). Mixed and homogeneous combinations were studied. Whenever the triple mutant construct was present, the BRET ratio was lower than that produced by the two wild-type receptor constructs. The lowest BRET ratio was observed for the two mutant receptors together, with the value not different from that of the level of BRET expected from nonspecific interactions (shown in the shaded area). Data are presented as the means ± S.E.M. of six independent experiments. *$p < 0.05$ compared with the BRET signal obtained from the tagged wild-type CCK receptor constructs.

BRET studies were performed with the Rlu- and YFP-tagged mutant CCK receptor constructs (Figure 7). As predicted, there was no significant BRET signal when these receptors were coexpressed on COS cells. Of interest, expressing such a construct along with wild-type CCK receptor resulted in a significant reduction of the receptor BRET signal, but a small signal was present. This may suggest that other faces of the external helical bundle also contribute to oligomerization, although the lipid-exposed face of TM VI is clearly very important.

*Morphological FRET Imaging*. In support of these BRET observations, morphological FRET localization studies demonstrated that wild-type CCK receptor homo-oligomers were present both at the cell surface and intracellularly in the biosynthetic pathway (Figure 8). However, for the mutant receptor with the alanine replacements within the lipid-exposed external face of TM VI, there was no such receptor–receptor interaction observed, with no FRET signal generated either intracellularly within the biosynthetic pathway or at the plasma membrane. Once again, this supports the BRET results, indicating the absence of specific interactions between this CCK receptor mutant and itself. This again confirms that lipid-exposed faces of key transmembrane segments of this receptor are responsible for the observed oligomerization.

*Saturation BRET*. Saturation BRET experiments were performed to further characterize the signal coming from the BRET experiments described above. This technique has been claimed as being able to distinguish a specific molecular interaction from a bystander effect of random approximation of donor and acceptor. As such, this may represent a tool to distinguish a conformational change increasing the distance from donor to acceptor from the true dissociation of a complex. The data are illustrated in Figure 9. In each case,

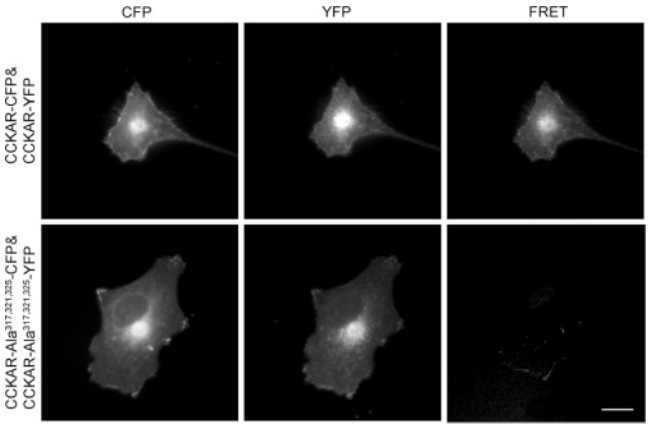


FIGURE 8: Morphological FRET imaging of CCK receptor and mutant CCK receptor oligomerization. Shown are the representative corrected microscopic images of fixed COS cells expressing CFP- and YFP-tagged wild-type (top row) or alanine mutant (bottom row) CCK receptor constructs. Images shown in the left, middle, and right columns represent background-subtracted CFP, YFP, and corrected FRET signals, respectively. Wild-type CCK receptors show a clear FRET signal generated at the cell surface and in intracellular compartments that were absent in the mutant receptor-expressing cells. The scale bar represents 25 $\mu$m.

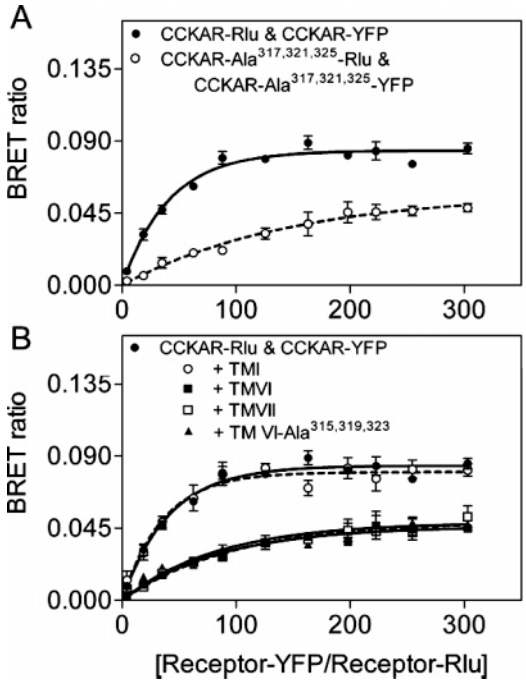


FIGURE 9: Saturation BRET data. Shown are the BRET saturation curves generated for pairs of Rlu- and YFP-tagged wild-type and mutant CCK receptor constructs (A) and the effects of competition with various TM peptides for the BRET signal generated by the wild-type A CCK receptor constructs (B). Data are represented as the means ± S.E.M of three independent experiments. Here, the peptide corresponding to TM I had no effect to disrupt the exponential curve, whereas the TM VI, TM VII, and the triple mutant peptide mutating the interhelical face resulted in curves similar to a linear regression fit.

the data were fit to the best single-exponential curve that provided the calculation of $BRET_{max}$ and $BRET_{50}$ values. The curves were also compared with a linear regression to determine whether the fit was significantly better for the exponential curve. In Figure 9A, where intact receptors were studied, the exponential curve provided a significantly better fit than the linear regression only for the wild-type CCK receptor ($BRET_{max} = 0.085 \pm 0.002$, $BRET_{50} = 29.4 \pm 2.2$). When the triple mutant CCK receptor construct in which the lipid-exposed face was modified was used for this experiment, the exponential fit was not better than the linear regression, making the determination of $BRET_{max}$ and $BRET_{50}$ values invalid. This supports the interpretation that wild-type CCK receptors oligomerize and that the mutation of the dimerization face of the CCK receptor disrupts its oligomerization. In Figure 9B, the same analyses were performed for the ability of varied TM peptides to affect the saturable BRET signal of the wild-type CCK receptor constructs. Here, the peptide corresponding to TM I had no effect to disrupt the exponential curve ($BRET_{max} = 0.080 \pm 0.002$, $BRET_{50} = 25.1 \pm 1.4$), whereas the TMVI, TMVII, and the triple mutant peptide mutating the interhelical face resulted in curves that were not statistically different from a linear regression fit. This again supports the interpretation that these peptides disrupted the oligomerized complex, rather than affecting its conformation.

## DISCUSSION

Examples of the oligomerization of G protein-coupled receptors have been reported at an accelerating pace and demonstrated using biochemical techniques such as co-immunoprecipitation and biophysical techniques such as BRET and FRET (*28*, *29*). Some of these articles have suggested that dimerization of these receptors can have functional significance, affecting ligand recognition, signal transduction, and receptor regulation (*3*, *4*, *30*, *31*). Because of the clear importance of this superfamily of receptors as pharmacologic targets, the existence of these complexes, their significance, and the molecular mechanisms responsible become key questions. In the current work, we have focused our efforts on the dimerization of the physiologically important type A CCK receptor, normally involved in various aspects of nutrient homeostasis, affecting pancreatic exocrine secretion, gut transit, and even post-cibal satiety (*32*). This receptor has previously been shown to exhibit constitutive dimerization that is subsequently disrupted by agonist binding (*14*). The molecular basis of this event and its functional significance were unclear prior to this article.

TM segments have been the focus of numerous experimental and theoretical analyses of oligomerization studies (*6*, *33*, *34*). In the current work, we have focused on the potential roles of these regions of the CCK receptor. We followed the experimental strategy initially reported by Hebert et al. (*13*) in which a synthetic peptide representing a TM segment of the $\beta_2$-adrenergic receptor was used to compete for and to inhibit the dimerization of that receptor, with disruption also interfering with agonist-stimulated biological activity. In this approach, by saturating the system with a replicate of a key interface for dimerization, the receptors were no longer able to efficiently find their partners to establish oligomeric complexes. There is extensive literature establishing the ability of TM segment peptides to associate with each other in a structurally sensitive manner (*33*).

Computational molecular modeling and bioinformatic approaches have been used to predict interaction interfaces for family A G protein-coupled receptors (*35*, *36*). This task has been complicated by the absence of high-resolution

structural data for the seven TM segment bundles, except for the inactive conformation of rhodopsin (*37*). Similarly, there are multiple possible models for the packing of such structures, including both contact dimers and oligomers as well as domain-swapped dimers. Evolutionary patterns, conserved residues, and correlated mutational events have been used in these studies to gain insights into the types of complexes that might be formed and the molecular mechanisms of their formation. In the current study, we examined TM segments I, II, V, VI, and VII, representing each of the interfaces previously implicated in the oligomerization of receptors in this family (*13*, *38*). Of these, only TM VI and TM VII disrupted the CCK receptor BRET signal. This was confirmed to represent the true dissociation of the bimolecular complex on the basis of the effect on the BRET saturation assay. It is of interest that one of the regions identified experimentally in the current article (TM VI) has also been a region identified using the computational approaches. TM IV, V, and VI have been identified as being potentially important in those studies (*9, 11*, *38*−*41*). CCK receptor TM VII was also identified as important in the current article, but its specific significance remains unclear.

TM VI of the $\beta_2$-adrenergic receptor was also the focus of the study by Hebert et al. (*13*), where using the synthetic TM VI peptide not only disrupted receptor dimerization but also inhibited agonist-induced signaling. This was replicated by Baneres and Parello (*40*) for the leukotriene B4 receptor BLT1 when they evaluated each of the seven TM segments using the same peptide competition strategy, finding that only TM segment VI inhibited receptor dimerization. That series of observations was also quite important because that receptor requires an intact homodimer to bind one molar equivalent of heterotrimeric G protein and, therefore, for functional activity (*40*). The experimental approach of disrupting specific faces of the transmembrane helix to examine which face might be responsible for the biological effect proved to be very powerful. It is notable that the lipid-exposed external face of TM VI of the CCK receptor turned out to be the face most relevant for dimerization. This, too, was confirmed using the BRET saturation assays. Using the nomenclature of Ballesteros and Weinstein (*18*), on the basis of the number of the TM segment and the residues relative to the most conserved residue within that segment arbitrarily assigned the position number of 50 (in TM VI this is a proline), this face includes residues 6.38, 6.42, and 6.46. Residue 6.42 of the $\beta_2$-adrenergic receptor was also identified experimentally as important for dimerization (*13*). Careful bioinformatic analysis also identified residue 6.42 as having a high likelihood of being at the interface of G protein-coupled receptor dimers (*36*). These predictions also correspond well with our current 3D model for the type A CCK receptor (*16*), which predicts that the same set of residues will likely be important for contact dimer formation.

There has been much discussion about the possibility of domain-swapped versus contact dimers of G protein-coupled receptors (*42*−*44*). The identification of the lipid-exposed face of TM VI of the CCK receptor as a critical interface for such complexes provides strong evidence for contact dimers of this receptor. This is, in fact, consistent with the simultaneous dual photoaffinity labeling data previously reported to establish a one-to-one stoichiometry of ligand occupation to receptor in CCK ligand−receptor complexes (*45*). This has been reflected in our current, best-refined model of this complex (*16*). Although the presence of contact dimers does not rule out the possibility of domain-swapped dimers of the CCK receptor, it is also easier to envision contact complexes rather than domain-swapped complexes being disrupted by agonist binding, as has been previously reported (*14*).

The importance of the lipid-exposed face of TM VI of the CCK receptor was further confirmed by intact receptor mutagenesis. Indeed, the receptor construct incorporating Ala residues to replace the residues normally at this face of TM VI was shown to eliminate the normally present CCK receptor BRET signal. In addition, morphological FRET studies also demonstrated the absence of resonance transfer for this CCK receptor mutant construct. These results for intact mutant CCK receptors and for TM VI peptides not only provide additional evidence for the formation of CCK receptor contact dimers but also provide additional support for our previously constructed type A CCK receptor models. We had no experimental constraint data to guide the specific positioning or orientation of TM VI in our previous modeling work; therefore, this was a poorly defined region in our structures. These current experimental results suggest that the placement and orientation of TM VI in our models are quite reasonable and allow us to constrain an additional region in the receptor model with greater confidence.

The intact receptor mutagenesis also provided an ideal opportunity to study the functional impact of CCK receptor oligomerization. Despite the interference with oligomerization, this receptor bound the natural ligand normally, signaled normally, and was internalized normally. This series of studies suggests that the contact dimers of the CCK receptor that are constitutively present on the surface of cells have no functional significance for the effect of its natural agonist ligand under normal physiologic conditions. However, recent studies have shown that oligomerization between the type A and type B CCK receptors and that between normal and misspliced receptors in this family have potentially important functional implications for cell growth and carcinogenesis (*15*, *46*). Assuming that the same molecular mechanism is involved in those oligomerization events, the role of the lipid environment may be a critical variable to study in the future.

## ACKNOWLEDGMENT

We thank Dr. Michel Bouvier for providing $\beta_2$-adrenergic receptor-Rlu and $\beta_2$-adrenergic receptor-YFP constructs and Dr. Cayle Lisenbee for his assistance with the morphological FRET studies. We thank Ms. Laura-Ann Bruins and Renee M. Happs for their excellent technical assistance and Ms. Evelyn Posthumus for her secretarial assistance.

## REFERENCES

1. Milligan, G., and White, J. H. (2001) Protein-protein interactions at G-protein-coupled receptors, *Trends Pharmacol. Sci. 22*, 513−518.
2. Dawson, J. P., Berger, M. B., Lin, C. C., Schlessinger, J., Lemmon, M. A., and Ferguson, K. M. (2005) Epidermal growth factor receptor dimerization and activation require ligand-induced conformational changes in the dimer interface, *Mol. Cell. Biol. 25*, 7734−7742.
3. Terrillon, S., and Bouvier, M. (2004) Roles of G-protein-coupled receptor dimerization, *EMBO Rep. 5*, 30−34.

4. Milligan, G. (2004) G protein-coupled receptor dimerization: function and ligand pharmacology, *Mol. Pharm. 66*, 1−7.
5. Bai, M. (2004) Dimerization of G-protein-coupled receptors: roles in signal transduction, *Cell. Signalling 16*, 175−186.
6. Filizola, M., Olmea, O., and Weinstein, H. (2002) Prediction of heterodimerization interfaces of G-protein coupled receptors with a new subtractive correlated mutation method, *Protein Eng. 15*, 881−885.
7. Lee, S. P., O'Dowd, B. F., Ng, G. Y., Varghese, G., Akil, H., Mansour, A., Nguyen, T., and George, S. R. (2000) Inhibition of cell surface expression by mutant receptors demonstrates that D2 dopamine receptors exist as oligomers in the cell, *Mol. Pharm. 58*, 120−128.
8. Canals, M., Marcellino, D., Fanelli, F., Ciruela, F., de Benedetti, P., Goldberg, S. R., Neve, K., Fuxe, K., Agnati, L. F., Woods, A. S., Ferre, S., Lluis, C., Bouvier, M., and Franco, R. (2003) Adenosine A2A-dopamine D2 receptor-receptor heteromerization: qualitative and quantitative assessment by fluorescence and bioluminescence energy transfer, *J Biol. Chem. 278*, 46741−46749.
9. Liang, Y., Fotiadis, D., Filipek, S., Saperstein, D. A., Palczewski, K., and Engel, A. (2003) Organization of the G protein-coupled receptors rhodopsin and opsin in native membranes, *J Biol. Chem. 278*, 21655−21662.
10. Fotiadis, D., Liang, Y., Filipek, S., Saperstein, D. A., Engel, A., and Palczewski, K. (2004) The G protein-coupled receptor rhodopsin in the native membrane, *FEBS Lett. 564*, 281−288.
11. Hebert, T. E., and Bouvier, M. (1998) Structural and functional aspects of G protein-coupled receptor oligomerization, *Biochem. Cell Biol. 76*, 1−11.
12. Milligan, G., Ramsay, D., Pascal, G., and Carrillo, J. J. (2003) GPCR dimerisation, *Life Sci. 74*, 181−188.
13. Hebert, T. E., Moffett, S., Morello, J. P., Loisel, T. P., Bichet, D. G., Barret, C., and Bouvier, M. (1996) A peptide derived from a beta2-adrenergic receptor transmembrane domain inhibits both receptor dimerization and activation, *J. Biol. Chem. 271*, 16384−16392.
14. Cheng, Z. J., and Miller, L. J. (2001) Agonist-dependent dissociation of oligomeric complexes of G protein-coupled cholecystokinin receptors demonstrated in living cells using bioluminescence resonance energy transfer, *J. Biol. Chem. 276*, 48040−48047.
15. Cheng, Z. J., Harikumar, K. G., Holicky, E. L., and Miller, L. J. (2003) Heterodimerization of type A and B cholecystokinin receptors enhance signaling and promote cell growth, *J. Biol. Chem. 278*, 52972−52979.
16. Ding, X. Q., Pinon, D. I., Furse, K. E., Lybrand, T. P., and Miller, L. J. (2002) Refinement of the conformation of a critical region of charge-charge interaction between cholecystokinin and its receptor, *Mol. Pharmacol. 61*, 1041−1052.
17. Mercier, J. F., Salahpour, A., Angers, S., Breit, A., and Bouvier, M. (2002) Quantitative assessment of beta 1- and beta 2-adrenergic receptor homo- and heterodimerization by bioluminescence resonance energy transfer, *J. Biol. Chem. 277*, 44925−44931.
18. Ballesteros, J. A., and Weinstein, H. (1992) Analysis and refinement of criteria for predicting the structure and relative orientations of transmembranal helical domains, *Biophys. J. 62*, 107−109.
19. Powers, S. P., Pinon, D. I., and Miller, L. J. (1988) Use of N, O-bis-Fmoc-D-Tyr-ONSu for introduction of an oxidative iodination site into cholecystokinin family peptides, *Int. J. Pept. Protein Res. 31*, 429−434.
20. Ulrich, C. D., Ferber, I., Holicky, E., Hadac, E., Buell, G., and Miller, L. J. (1993) Molecular cloning and functional expression of the human gallbladder cholecystokinin A receptor, *Biochem. Biophys. Res. Commun. 193*, 204−211.
21. Harikumar, K. G., Clain, J., Pinon, D. I., Dong, M., and Miller, L. J. (2005) Distinct molecular mechanisms for agonist peptide binding to types A and B cholecystokinin receptors demonstrated using fluorescence spectroscopy, *J. Biol. Chem. 280*, 1044−1050.
22. Harikumar, K. G., Pinon, D. I., Wessels, W. S., Prendergast, F. G., and Miller, L. J. (2002) Environment and mobility of a series of fluorescent reporters at the amino terminus of structurally related peptide agonists and antagonists bound to the cholecystokinin receptor, *J. Biol. Chem. 277*, 18552−18560.
23. Munson, P. J., and Rodbard, D. (1980) Ligand: a versatile computerized approach for characterization of ligand-binding systems, *Anal. Biochem. 107*, 220−239.
24. Hadac, E. M., Ghanekar, D. V., Holicky, E. L., Pinon, D. I., Dougherty, R. W., and Miller, L. J. (1996) Relationship between native and recombinant cholecystokinin receptors: role of differential glycosylation, *Pancreas 13*, 130−139.
25. Grynkiewicz, G., Poenie, M., and Tsien, R. Y. (1985) A new generation of Ca2+ indicators with greatly improved fluorescence properties, *J. Biol. Chem. 260*, 3440−3450.
26. Harikumar, K. G., Puri, V., Singh, R. D., Hanada, K., Pagano, R. E., and Miller, L. J. (2005) Differential effects of modification of membrane cholesterol and sphingolipids on the conformation, function, and trafficking of the G protein-coupled cholecystokinin receptor, *J. Biol. Chem. 280*, 2176−2185.
27. Harikumar, K. G., Morfis, M. M., Lisenbee, C. S., Sexton, P. M., and Miller, L. J. (2006) Constitutive formation of oligomeric complexes between family B G protein-coupled vasoactive intestinal polypeptide and secretin receptors, *Mol. Pharmacol. 69*, 363−373.
28. Gomes, I., Filipovska, J., Jordan, B. A., and Devi, L. A. (2002) Oligomerization of opioid receptors, *Methods 27*, 358−365.
29. Pfleger, K. D., and Eidne, K. A. (2005) Monitoring the formation of dynamic G-protein-coupled receptor-protein complexes in living cells, *Biochem. J. 385*, 625−637.
30. Rashid, A. J., O'Dowd, B. F., and George, S. R. (2004) Minireview: Diversity and complexity of signaling through peptidergic G protein-coupled receptors, *Endocrinology 145*, 2645−2652.
31. Salahpour, A., Angers, S., and Bouvier, M. (2000) Functional significance of oligomerization of G-protein-coupled receptors, *Trends Endocrinol. Metab. 11*, 163−168.
32. Mutt, V. (1981) Additional observations on cholecystokinin and the vasoactive intestinal polypeptide, *Peptides 2*, 209−214.
33. MacKenzie, K. R., Prestegard, J. H., and Engelman, D. M. (1997) A transmembrane helix dimer: structure and implications, *Science 276*, 131−133.
34. Lemmon, M. A., Flanagan, J. M., Treutlein, H. R., Zhang, J., and Engelman, D. M. (1992) Sequence specificity in the dimerization of transmembrane alpha-helices, *Biochemistry 31*, 12719−12725.
35. Filizola, M., and Weinstein, H. (2002) Structural models for dimerization of G-protein coupled receptors: the opioid receptor homodimers, *Biopolymers 66*, 317−325.
36. Filizola, M., and Weinstein, H. (2005) The study of G-protein coupled receptor oligomerization with computational modeling and bioinformatics, *FEBS J. 272*, 2926−2938.
37. Palczewski, K., Kumasaka, T., Hori, T., Behnke, C. A., Motoshima, H., Fox, B. A., Le Trong, I., Teller, D. C., Okada, T., Stenkamp, R. E., Yamamoto, M., and Miyano, M. (2000) Crystal structure of rhodopsin: A G protein-coupled receptor, *Science 289*, 739−745.
38. Hernanz-Falcon, P., Rodriguez-Frade, J. M., Serrano, A., Juan, D., del Sol, A., Soriano, S. F., Roncal, F., Gomez, L., Valencia, A., Martinez, A. C., and Mellado, M. (2004) Identification of amino acid residues crucial for chemokine receptor dimerization, *Nat. Immunol. 5*, 216−223.
39. George, S. R., Lee, S. P., Varghese, G., Zeman, P. R., Seeman, P., Ng, G. Y., and O'Dowd, B. F. (1998) A transmembrane domain-derived peptide inhibits D1 dopamine receptor function without affecting receptor oligomerization, *J. Biol. Chem. 273*, 30244−30248.
40. Baneres, J. L., and Parello, J. (2003) Structure-based analysis of GPCR function: evidence for a novel pentameric assembly between the dimeric leukotriene B4 receptor BLT1 and the G-protein, *J. Mol. Biol. 329*, 815−829.
41. Guo, W., Shi, L., Filizola, M., Weinstein, H., and Javitch, J. A. (2005) Crosstalk in G protein-coupled receptors: Changes at the transmembrane homodimer interface determine activation, *Proc. Natl. Acad. Sci. U.S.A. 102*, 17495−17500.
42. Gouldson, P. R., Snell, C. R., Bywater, R. P., Higgs, C., and Reynolds, C. A. (1998) Domain swapping in G-protein coupled receptor dimers, *Protein Eng. 11*, 1181−1193.
43. Gouldson, P. R., Higgs, C., Smith, R. E., Dean, M. K., Gkoutos, G. V., and Reynolds, C. A. (2000) Dimerization and domain swapping in G-protein-coupled receptors: a computational study, *Neuropsychopharmacology 23*, S60−S77.
44. Gouldson, P. R., Dean, M. K., Snell, C. R., Bywater, R. P., Gkoutos, G., and Reynolds, C. A. (2001) Lipid-facing correlated mutations and dimerization in G-protein coupled receptors, *Protein Eng. 14*, 759−767.
45. Hadac, E. M., Ji, Z., Pinon, D. I., Henne, R. M., Lybrand, T. P., and Miller, L. J. (1999) A peptide agonist acts by occupation of

a monomeric G protein-coupled receptor: dual sites of covalent attachment to domains near TM1 and TM7 of the same molecule make biologically significant domain-swapped dimerization unlikely, *J. Med. Chem. 42*, 2105−2111.

46. Cheng, Z. J., Harikumar, K. G., Ding, W. Q., Holicky, E. L., and Miller, L. J. (2005) Analysis of the cellular and molecular mechanisms of trophic action of a misspliced form of the type B cholecystokinin receptor present in colon and pancreatic cancer, *Cancer Lett. 222*, 95−105.
47. *DINO* (2001) Visualizing Structural Biology, http://www.dino3d.org.
48. Sanner, M. F., Olson, A. J., and Spehner, J. C. (1996) Reduced surface: an efficient way to compute molecular surfaces, *Biopolymers 38*, 305−320.

BI061107N